Journal Pre-proof

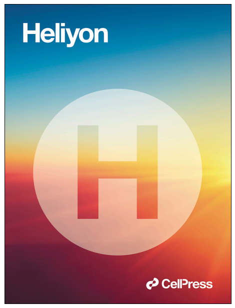

Optimizing Domestic Energy Management with a Wild Mice Colony-Inspired Algorithm: Enhancing Efficiency and Coordination in Smart Grids through Dynamic Distributed Energy Storage

Liang Wang, Dajun Li

PII: S2405-8440(24)11493-4

DOI: https://doi.org/10.1016/j.heliyon.2024.e35462

Reference: HLY 35462

To appear in: *HELIYON*

Received Date: 14 April 2024

Revised Date: 27 July 2024

Accepted Date: 29 July 2024

Optimizing Domestic Energy Management with a Wild Mice Colony-Inspired Algorithm: Enhancing Efficiency and Coordination in Smart Grids through Dynamic Distributed Energy Storage

Liang Wang[1] and Dajun Li[2,*]

[1] School of Mechanical Engineering, Southeast University, Nanjing 211189, Jiangsu, China

[2] School of Mechanical and Electrical Engineering, Chengdu University of Technology, Chengdu 610000, Sichuan, China

Abstract

Energy management (EM) is a critical strategy that spans the production and consumption of electricity, enhancing the stability of the electricity network. Smart grid technology significantly improves the electrical system's energy efficiency (EE), facilitating a transformation from a conventional power grid (PG) to a smart PG. This paper presents a key strategy for modeling the EE of the smart grid tailored to domestic demand, establishing smart coordination between domestic demand, energy production, and storage to reduce energy waste and costs. Our model integrates various energy sources, including renewable energy (RE), photovoltaic (PV) systems, wind power, and an energy storage system (ESS), interconnected with the PG. The model's structure ensures the coordinated flow of electricity in a residential house through an optimal control method (OCM). To develop a robust closed-loop control model, we employ Demand Response (DR) schemes within the Real-Time Electricity Pricing (RTEP) framework. We construct a dynamic model of the ESS to compute the System Performance Index (SPI), corresponding to energy costs. To enhance our model, we introduce a Dynamic Distributed Energy Storage Strategy (DDESS). Additionally, we introduce a novel optimization algorithm inspired by the behavioral patterns of wild mice, called the Wild Mice Colony (WMC). By analyzing the targeted and advantageous behaviors of wild mice in colonies, we propose that these behaviors can serve as a model for addressing complex, uncertain problems. This strategy is highly advantageous, capable of reducing total energy consumption (EC) from the main grid by over 100% of the load demand, optimizing the energy system, and ensuring synchronization. The performance of DDESS optimizes energy flow (EF) during the repayment plan, leading to minimized EC costs from the PG.

[*] Corresponding Author
E-mail Addres: lidajun@cdut.edu.cn

Keywords: Renewable energy, Dynamic distributioned energy storage, Energy efficiency, Optimization algorithm.

List of Abbreviations

BESS	Battery Energy Storage System
CB	Battery Capacity
Cb	Energy Storage System Cost
Cgr	Cost of Energy Consumption from Power Grid
Cop	Opportunity Load Cost
CH	Colony Head
CEPB	Consumer Energy Payback
CEEPB	Consumer End Energy Payback
DER	Distributed Energy Resource
DES	Distributed Energy system
DDESS	Dynamic Distributed Energy Storage Strategy
DR	Demand Response
DG	Distributed Generation
EC	Energy Consumption
EF	Energy Flow
EE	Energy Efficiency
EM	Energy Management
ESS	Energy Storage System
EMSs	Energy management systems
Ha	Battery Autonomy hour
OCM	Optimal Control Method
PG	Power Grid
PrDER	Renewable Energy Pricing
Prgr	Price of load paid to PG
PV	Photovoltaic
RE	Renewable Energy
RERs	Renewable Energy Resources
RTEP	Real-Time Electricity Pricing
SOC	State of Charge
SPI	System Performance Index
WT	Wind Turbine

WMC Wild Mice Colony

1. Introduction

In recent decades, the growing complexity of urban power grids has necessitated the deployment of advanced real-time monitoring, control, and protection systems to enhance overall electrical system efficiency [1-3]. The integration of Renewable Energy Resources (RERs), which are characterized by production uncertainties, presents challenges to power flow quality [4-6]. EM has emerged as a pragmatic solution to address these challenges within the power grid. Smart grid technology has proven pivotal by offering solutions to a multitude of current grid issues. It effectively addresses scheduling conflicts and cross-sector power transmission challenges through its intelligent electrical system design. By incorporating RERs, optimizing transmission and distribution network efficiency, and meeting demand requirements for enhanced reliability and quality supply, the smart grid establishes a framework to manage and mitigate grid instability, operational uncertainties, and proactive planning needs. Real-time control implementation is central to smart grid technology, enhancing grid efficiency, security, and reliability. Operating seamlessly across both large-scale and small-scale power generation and consumption, the smart grid facilitates adaptive enhancements in Distributed Generation (DG) and ESSs [7]. Furthermore, by reducing overall electricity costs, energy efficiency within smart grid systems ensures coordinated electrical flow between energy supply and demand. Contemporary methodologies have been employed to effectively manage EF in various electrical systems, spanning residential to commercial applications [8–16]. A noteworthy contribution involves designing an OCM for residential use within an advanced metering infrastructure, intelligently managing variable load demands [8]. The proposed model, aimed at enhancing EC efficiency, integrates RERs. Additionally, an intelligent system is introduced to evaluate residential energy cost savings, taking into account three devices and four pricing schemes [17]. Employing a two-stage optimization strategy based on mixed-integer linear programming, the model initially plans electricity usage for each device and subsequently estimates the energy price for each device.

Additionally, a decentralized strategy for coordinating load consumption in residential houses based on DR is introduced [18]. This plan implements a clever method that lowers end consumers' power costs without sacrificing their confidentiality or satisfaction. The model integrates multiple independent home EMSs within an intelligent distribution system, which includes energy distribution services merging power and communication networks. Interestingly, these systems do not incorporate renewable energy sources like solar and wind. RERs can be effectively integrated into the electric grid thanks to the advancement of the smart grid. A load reduction approach is suggested [19] that makes use of a multi-agent system and the personal decision technique. The strategy focuses on coordinating the upstream network, RERs, and DR schemes to minimize stress caused by peak loads on the feeder. Furthermore, an intelligent home energy coordinating system is shown [20], which uses intelligent meters to connect small-scale PV power to the metropolitan grid. Operating in two stages based on network operator decisions and intelligent scheduling, the approach optimizes energy demand from the PG, thereby enhancing home electricity consumption efficiency. Residential EM in a smart grid environment addresses the challenges posed by dynamic electricity pricing schemes, enabling users to navigate complex pricing structures. The coordination of residential EFs further facilitates the integration of sustainable energy sources. Effectively managing EF for suburban homes presents challenges, influenced by diverse load demands in the residential sector, their operational schedules, and the integration of RERs in the power distribution system. Smart grid technologies offer strategies to coordinate EFs for residential consumers, aiming to minimize EC and enhance system efficiency by considering load variations. Nevertheless, there remains a weakness in residential power flow modeling, especially when it comes to using flexible energy storage in conjunction with a RTEP-based cost function that accounts for the opportunity cost of energy. Addressing this gap involves developing and implementing a robust OCM to coordinate EF between production and usage in a residential intelligent house, utilizing smart metering. This model not only empowers end users to optimally sell energy to suppliers but also involves designing a dynamic algorithm for Distributed Energy Storage (DES) based on closed-loop OCM. An RTEP scheme with hourly energy pricing for various energy-generating components is implemented by the algorithm. The major objective of the suggested approach is to create a SPI that penalizes the PG for energy usage while preserving earnings from other energy production sources, such as opportunity energy and DERs like photovoltaic (PV) systems, wind turbines (WTs), and DES. In a hypothetical implementation, system improvement analysis is conducted by methodically varying the battery's initial state of charge (SOC) within predetermined minimum/maximum amounts. Using potential savings ranging from 61 to 157% of total energy expenses for PG usage, the DDESS model proves its efficacy in reducing energy consumption. The energy production system, the energy control system, and the ESS are three primary components of smart grid technologies used for residential energy coordination. Residential PV, micro-WTs, and supply utilities or the main grid are examples of energy production [21].

Customers use home appliances with a variety of load requirements, including thermal and non-thermal loads as well as flexible and non-flexible loads. In this case, buyers might be energy providers or consumers. At the moment, electric cars and battery storage systems dominate the domestic EC market [22]. EFs in residential settings have been managed using various tactics. One noteworthy method involves creating a multi-objective mixed-integer nonlinear program framework for DR via the EMS of an intelligent house. This model considers residential users' thermal comfort zones and energy savings. To guarantee heating system operation based on thermal demand and user comfort levels, it creates and assesses a RTEP plan across various operating conditions. This ensures optimal device and unit management, with various heating and cooling conditions evaluated for resilience and efficiency. In residential applications, DR is investigated as a potential method for system air conditioning load evaluation. The system creates a model based on home air conditioning, in which indoor and outdoor temperatures determine the overall system power. By incorporating DR strategies, the system predicts residential air conditioning loads, ensuring effective regulation and enhancing network operation economy and resource capability.

In light of a high penetration rate for residential PV systems and an RTEP program, a unique home emergency management system is proposed. This system creates a sophisticated adaptive thermal comfort model and an operating model for home appliances to measure and assess users' interior thermal comfort levels. The system design uses a novel intelligent self-assembly algorithm inspired by biology to solve the energy source scheduling challenge. Simulation research results show that the proposed approach improves residential building automation and responds efficiently to RE output and RTEP. Furthermore, an efficient EMS for a home microgrid is provided [12]. This model incorporates an optimization strategy to address various aspects of the designed system, including distributed power and heat production, heat transfer, thermal interactions with environmentally friendly residential buildings, and arranging load potentials using household appliances with system constraints. The suggested approach ensures household comfort while coordinating EM at every level, from supply to demand. To reduce overall energy expenses, a DR method is used to design another residential EMS [23]. The system uses a Lyapunov-based cost reduction technique in conjunction with a decentralized online control algorithm to coordinate many residential households. This technique maximizes EF throughout the entire electrical system by utilizing the DR framework. If there is flexibility and a delay in energy demand, the model can lower the system's overall power usage. Essential and flexible demands are the two categories into which households are divided [24]. The intelligent coordination of EC, complicated demands, and operational delays is the aim of this method. The SPI is greatly impacted by the flexible load, which is defined by demands that are both delay-tolerant and delay-sensitive. In response, a centralized algorithm is used to construct an adaptive dynamic planning model that uses optimization to make decisions that minimize overall energy costs and operational delays for changeable needs.

Under the DR approach, an additional intelligent residential EM plan is created [25]. By offering a different approach to energy generation from RE technologies for residential use, this model seeks to meet future demand. An SPI that coordinates various load types according to the electricity price horizon is implemented by the system algorithm. In addition, under a potential optimization strategy, a domestic energy center with RE, natural gas generation, electric vehicles, and a storage system is suggested [26]. To maximize system efficiency, this model best handles uncertainty associated with solar panels and synchronization of fluctuating load outcomes. To increase system efficacy, a different energy coordination control architecture is created [26, 27]. This model detects customer behavior from real-time total consumption by utilizing hidden Markov modeling techniques in conjunction with the DR approach. The system formulates an optimization method for scheduling and managing user devices by taking into account a dynamic activity detection model. In addition, an economic dispatch method is suggested to assess the effect of the load tariff and the ideal storage capacity [28]. Since battery storage is industry standard for renewable energy applications in the residential market, it may significantly reduce total operating costs by guaranteeing a complete supply to demand. To coordinate load relationships among the PG, electric car, and RE for home power consumption, a stochastic multi-stage decision-making approach is provided [29]. The power management of a smart home is optimized using a stochastic dynamic programming approach in this model. The algorithm was implemented to enhance its complexity and effectiveness in managing energy costs. To achieve ideal cost-saving behavior, the model utilizes an opportunity strategy with storage systems, including electric vehicles and batteries. The SPI is calculated for these interconnected operations, accounting for the impact of opportunity energy gaps. As a result, our study presents a sophisticated method for developing a flexible and comprehensive communication strategy [30]. In this paper, EM is detailed as a coordination strategy within the electrical load system, aimed at improving load flow. We have devised an optimal EF control strategy that integrates dynamic distributed storage feedback within a RTEP framework and a prepaid tariff system. This model incorporates dynamic pricing into the RTEP scheme, thus enhancing demand-side energy management. Given the growing complexity of energy systems due to increased demand, limited production, and global electricity access challenges, the integration of RERs addresses several technical issues. As mentioned, the proposed model acts as an intelligent coordination scheme via the dynamic energy storage system (ESS) model, utilizing system EF data. Additionally, it considers battery discharge depth variations based on the state of charge (SOC) and applies an optimal control method (OCM) to manage the overall system behavior. In this article, we present several key contributions and novelties in the field of EM for smart grids:

1. Optimal EF Control Strategy: An optimal EF control strategy is introduced, leveraging dynamic distributed storage feedback within the framework of a RTEP scheme coupled with a prepaid tariff structure.
2. Dynamic Pricing Integration: The model incorporates an electric dynamic pricing plan within the RTEP framework, integrating demand-side energy management into the overall strategy.
3. Incorporation of RERs: The model incorporates RERs to address the escalating complexity of the energy system due to increasing energy demand, insufficient energy production, and limited electricity grid access.
4. Intelligent Coordination Scheme: An intelligent coordination scheme is implemented through the dynamic model of the ESS, utilizing system energy flow data to optimize performance.
5. Battery Discharge Management: The model accounts for variations in battery discharge depth as a function of SOC, facilitating the OCM to effectively manage the overall behavior of the system.
6. Algorithm and Model Simplification: The proposed model is followed by presenting algorithms and relationships (including the rat colony algorithm) to simplify and optimize the problem.

2. Formulation of Energy Management System

Figure 1 illustrates a schematic representation of the proposed model's system design. The primary objective of this system is to effectively manage energy production in response to residential energy demand. The integration of a DER within the system transforms it into a grid-connected microgrid. The coordination facilitated by the DDESS enhances energy flexibility on the consumer side. Through the devised energy coordination structure, the model has the capability to channel surplus energy generated by the DER into the main grid. Notably, opportunity energy, originating from the DER, is taken into account when energy demand is lower than that supplied by the DER. As illustrated in Figure 1, when opportunity energy is absent, the current energy status in the system is delineated by Equation (1). Conversely, when the opportunity energy exceeds zero, the EF within the framework is expressed by Equation (2). In this scenario, it is assumed that the load generated by the DER surpasses the load demand at a specific time t, managed by the DDESS.

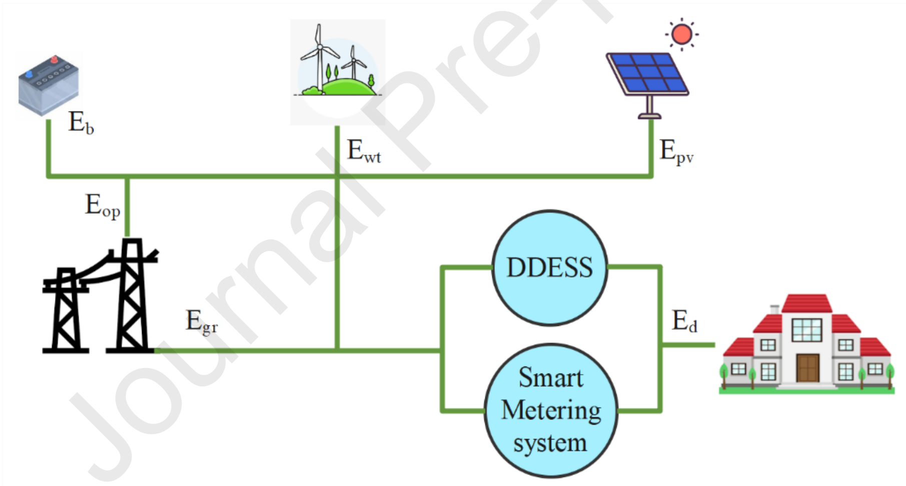

Figure 1: Intelligent energy coordination based on dynamic DES optimal control

The energy components in the system are represented by various variables: $E_d(t)$ denotes movement of energy on demand side., $E_{wt}(t)$ stands for energy produced by WT, $E_{pv}(t)$ corresponds to energy produced by the PV system, $E_{gr}(t)$ signifies energy supplied by the power company, and $E_{dc}(t)$ represents discharge energy from storage system, equating to $E_d(t)$ when $E_d(t)$ is less than zero. Any extra DER energy is referred to as opportunity energy in Equation (2) when it reaches the critical level needed to fulfill the entire load demand at a given moment. Equation (3) provides a mathematical expression for this, in which opportunity energy is denoted by E_{op}. Notably, opportunity energy is minimal when the battery is charging. As seen in Figure 1, the energy production of the EF via the main grid is dependent upon opportunity energy from the DER, which is supplied to the user by the distribution system operator. Equations (4) and (5) capture this relationship, where E_{ug} stands for the

EF in the PG. The energy pricing is specified within the scope of the proposed model as a prepaid tariff, incorporating a RTEP system as previously explained [30].

$$E_d(t) = E_{wt}(t) + E_{pv}(t) + E_{gr}(t) + E_{dc}(t) \quad (1)$$

$$E_d(\mathrm{t}) = E_{wt}(t) + E_{pv}(t) + E_{dc}(t) \quad (2)$$

$$E_{op}(t) = E_{wt}(t) + E_{pv}(t) + E_{dc}(t) - E_d(t) \quad (3)$$

$$E_{ug}(\mathrm{t}) = E_{gr}(t) \quad if \quad E_{op}(t) = 0 \quad (4)$$

$$E_{ug}(\mathrm{t}) = -E_{op}(t) \quad if \quad E_{gr}(t) = 0 \quad (5)$$

2.1. Energy storage system, WT and PV

In power system applications, incorporating a Battery Energy Storage System (BESS) is recognized as a pivotal strategy for enhancing operational efficiency. BESS is essential for synchronizing the flow of electricity, controlling voltage and frequency, and increasing the electrical system's immediate capacity. To articulate a dynamic battery model for improvement purposes, several relationships come into play.

Expressing the SOC at a given time ttt as SOC (t), where SOC (0) signifies the initial SOC, the dynamic model of energy storage is formulated in Equation (6). In this equation, E_{ch}(t) and E_{disc}(t) represent the energy flow into and out of the battery during charging and discharging periods, respectively. Parameters n_c and n_d signify charging and discharging coefficients, respectively. The dynamic strategy updates the initial SOC to the subsequent SOC value at each time instance.

In the context of battery charging modes, Equation (6) is reformulated as the first equation in Equation (7), where n_{ch} is the battery charge coefficient. The battery capacity is represented by C_B, while the inverter ratio is n_{inv}. During discharge, Equation (3) is employed to describe the stored load of the battery. Equation (6) is further recast as the second equation in Equation (7), where ndisc represents the battery discharge coefficient. The battery capacity is also determined by Equation (8), with H_a denoting the battery autonomy hour and $E_{d.avg}$ signifying average hourly demand.

Notably, battery capacity undergoes changes over time, a factor incorporated by considering SOC during charging (the first equation) and discharge (the second equation) in Equation (7). Crucially, charge and discharge parameters, described in Equations (11) and (12), are time-dependent, making battery capacity a variable over time due to the depth of discharge.

The energy generated by the WT relies on electrical power production, as denoted by Equation (13). In this equation, P_{wt} represents the average power demand, n_{wt} is WT efficiency, ρ_{air} is air density, C_p is WT's performance coefficient, A is the swept area of the turbine, and V is average wind speed. When operating within a specified time horizon N, the WT's energy output can be calculated using Equation (14), where ttt denotes sample time, and Δt represents the time change within the chosen time horizon N. For the PV system, its power production is governed by Equation (15), indicating that load generated by a PV is proportional to its surface area and the received solar radiation. Here, P_{pv} signifies the power produced by PV, n_{pv} is PV system efficiency, A_{pv} is the active area of PV, and I is solar radiation at the PV panel. The energy produced by the PV system over a designated time horizon N can be determined using Equation (16) [31]:

$$SOC(t) = SOC(0) + n_c.E_{ch}(t) - n_d.E_{disc}(t) \tag{6}$$

$$\begin{aligned} \mathrm{SOC}(\mathrm{t}+1) = \mathrm{SOC}(\mathrm{t}) + \frac{\left(E_{pv}(t) + E_{wt}(t) - E_d(t)\right).n_{ch}}{n_{inv}.CB} \\ = SOC(t) - \frac{(E_{op}(t) + E_d(t) - E_{pv}(t) - E_{wt}(t)}{n_{dise}.n_{inv}.CB} \\ = SOC(t) + n_c(t).E_{ch}(t) - n_{dc}(t).E_{disc}(t) \end{aligned} \tag{7}$$

$$\mathrm{CB} = \frac{Ha.E_{d.avg}}{n_{inv}.n_{disc}.(100 - SOC(t)} \tag{8}$$

$$E_{ch}(\mathrm{t}) = E_{pv}(t) + E_{wt}(t) - E_d(t) \tag{9}$$

$$E_{disc}(\mathrm{t}) = E_{op}(t) + E_d(t) - E_{pv}(t) - E_{wt}(t) \tag{10}$$

$$n_c(\mathrm{t}) = \frac{n_{ch}}{n_{inv}.CB(t)} \tag{11}$$

$$n_{dc}(\mathrm{t}) = \frac{1}{n_{disc}.n_{inv}.CB(t)} \tag{12}$$

$$P_{wt} = \frac{6}{\pi}.n_{wt}.\rho_{air}.C_p.A.V \tag{13}$$

$$W_{wt}(t) = \frac{6}{\pi}.n_{wt}.\rho_{air}.C_p.A.\Delta t.\sum_{t=1}^{N} V(t) \tag{14}$$

$$P_{pv} = n_{pv}.A_p.I \tag{15}$$

$$E_{pv}(\mathrm{t}) = n_{pv}.A_p.\Delta t\sum_{t=1}^{N} I(t) \tag{16}$$

3. Optimization and Cost Reduction in DDESS

The DDESS is meticulously crafted with the overarching goal of optimizing the EF within the system, primarily resulting in a substantial reduction in energy costs sourced from the PG. Beyond cost reduction, this model is strategically devised to maximize EF on the DER side, creating a valuable opportunity to contribute excess energy back to the grid. The holistic system design integrates a SPI for every element, as vividly illustrated in Figure 2 [12]. This index serves as a comprehensive metric for evaluating and enhancing the performance of SPI elements. Notably, the entire structural framework is anchored in a RTEP scheme, incorporating time frame rates for electricity. This dynamic pricing approach ensures that the system operates efficiently in response to the fluctuating costs of electricity. The use of prepaid tariffs adds an additional layer of flexibility and responsiveness to the system, enabling it to adapt swiftly to market dynamics.

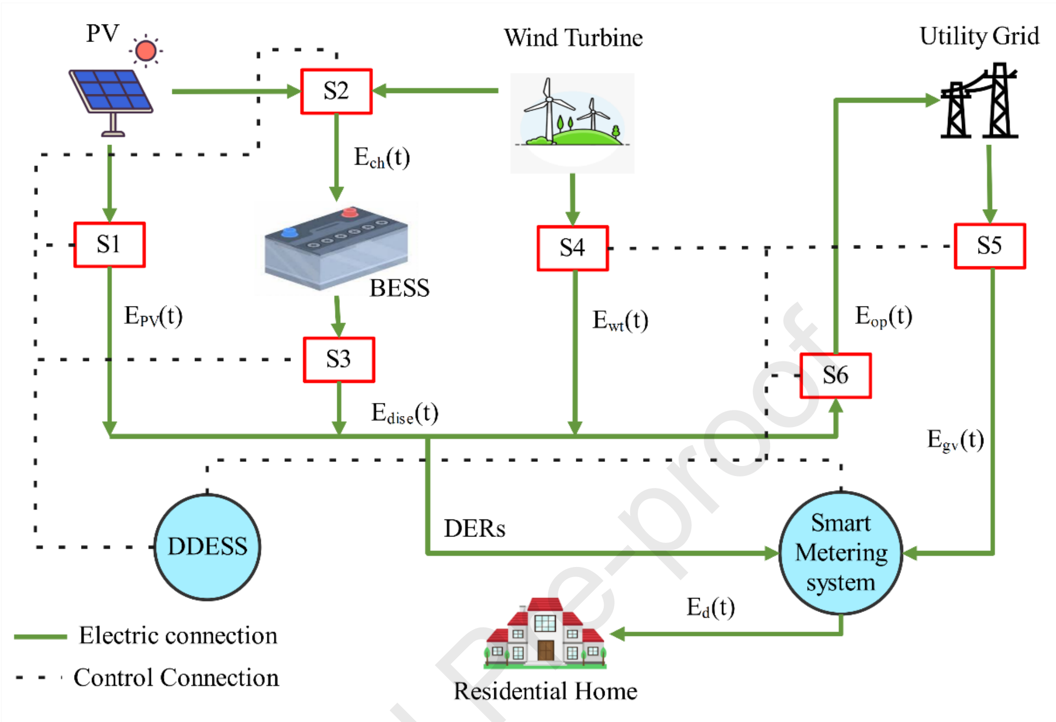

Figure 2: Schematic of energy coordination of residential house DDESS

The OCM's primary objective is to efficiently coordinate switching systems (S1, S2, S3, S4, S5, and S6). Switching within the context of the DDESS is pivotal for optimizing energy flow and enhancing system efficiency. It involves the strategic control and coordination of electrical energy between different sources, loads, and storage systems in real-time. The primary goal is to facilitate seamless transitions and maximize the utilization of DERs, such as solar and wind power, while minimizing costs from the utility grid. Integrated within the DDESS framework, switching systems like S1 to S6 enable adaptive management of energy resources, responding dynamically to fluctuating energy demand and renewable energy generation. This capability not only improves grid stability and reliability but also supports sustainable energy practices by promoting the efficient use of renewable resources and energy storage technologies. Through advanced control strategies and real-time monitoring, switching ensures that energy flows are optimized according to operational conditions and economic considerations, contributing to a more resilient and cost-effective energy infrastructure.

In an electric framework relying solely on the PG supply, the cost of EC within a specified time horizon N is quantified by Equation (17). Here ,C_{gr} represents the cost of EC from the PG when the load possibility is considered minimal, and Pr_{gr} signifies the price of the load paid to the PG. It's noteworthy that this price combines the current electricity pricing plan with prepaid electricity tariffs. For DERs, the cost of EC on the demand side is scrutinized, and the opportunity cost of the load utilizes the structure outlined in Equation (17). In this scenario, RTEP merges with RE pricing, denoted by $Pr_{DER.}$ Equations (18)-(21) delineate the various energy costs associated with DER, covering the wind turbine (C_{wt}), photovoltaic system (C_{pv}), distributed energy storage (C_b), and opportunity load cost (C_{op}). The SPI of the DDESS relies on Equations (17)-(21). The objective function aims to establish an optimal structure for a closed-loop model, as articulated in Equation (22), where $k_{j,}$ represents the SPI. Here, k denotes the time sample allocated within the control horizon of the system (Nc), and j signifies the level or temporal changes within the control horizon. The equality in Equation (22) demonstrates that the designed model, as depicted in Figures 1 and 2, minimizes the cost of load sourced from the PG while concurrently maximizing the utilization of energy derived from DER. Furthermore, the opportunity cost outlined in Equation (21) can be adjusted within the electricity price function of the PG. Consequently, the SPI formulated in Equation (22) can be redefined as Equation (23), offering a comprehensive perspective on the optimized EM objectives of the system [12].

$$C_{gr}(t) = P_{r_{gr}} \sum_{t=1}^{N} E_{gr}(t) \tag{17}$$

$$C_{wt}(t) = P_{r_{DER}} \sum_{t=1}^{N} E_{wt}(t) \tag{18}$$

$$C_{pv}(t) = P_{r_{DER}} \sum_{t=1}^{N} E_{PV}(t) \tag{19}$$

$$C_{b}(t) = P_{r_{DER}} \sum_{t=1}^{N} E_{b}(t) \tag{20}$$

$$C_{op}(t) = P_{r_{DER}} \sum_{t=1}^{N} E_{op}(t) \tag{21}$$

$$\min J(K) = \sum_{k=1}^{N} \sum_{j=1}^{N_c=k} \left[C_{ug,k_j}(k) - C_{wt,k_j}(k) - C_{pv,k_j}(k) - C_{b,k_j}(k) - C_{op,k_j}(k)\right] \tag{22}$$

$$\min J(K) = \sum_{k=1}^{N} \sum_{j=1}^{N_c=k} \left[p_{r_{gr}}\left(E_{ug,k_j}(k) - E_{op,k_j}(k)\right) - p_{r_{DER}} E_{DER,k_j}(k)\right] \tag{23}$$

3.1. DDESS Constraints

Derived from the SPI outlined in Equations (22) and (23), the functions of the DDESS can be systematically defined. The interplay of load within the system encapsulates its constraints, as visually represented in the figures. Concerning EC, these limitations are intricately linked to all the components contributing to load demand [32]. The bounds on EC manifest as a function of Equation

(1), treated as an equality constraint and expressed over the sample time 'k' in Equation (24). Building upon this constraint (24), the restrictions on power network capabilities can be elucidated through Equation (25). Similarly, the constraints on PV and WT systems are outlined in Equations (26) and (27), respectively. The DES system, instrumental in determining the SOC and EF limits within the battery, establishes constraints on EF during both charging and discharging periods. Consequently, the limitations on the battery are succinctly summarized in Equations (28) and (29). It's worth noting that EF limits on the battery can vary from negative to positive values, contingent upon the operational mode of the ESS. However, for the sake of the performance formula described in Equations (23) and (24), a positive assumption is made in this instance. Additionally, the system implementation incorporates extra constraints, specifically opportunity constraints based on Equations (4) and (5). The lower and upper constraints of the system are assigned to the EF parameters, as depicted in Figure 2. The DDESS calculations hinge on the implementation of Equations (22) and (23), subject to all the aforementioned restrictions delineated in this section. This comprehensive approach ensures that the optimization process considers and adheres to the multifaceted constraints imposed on the system, resulting in a robust and effective EM strategy.

$$E_d(k) = E_{pv}(k) + E_{wt}(k) + E_{disc}(k) + E_{gr}(k) \tag{24}$$

$$E_{gr_{max}}(\mathrm{k}) \leq E_{d_{max}}(k) \quad , \quad E_{gr_{min}}(\mathrm{k}) \geq 0 \tag{25}$$

$$E_{pv}(\mathrm{k}) \leq E_{pv_{max}}(k) \quad , \quad E_{pv_{min}}(\mathrm{k}) \geq 0 \tag{26}$$

$$E_{wt}(\mathrm{k}) \leq E_{wt_{max}}(k) \quad , \quad E_{wt_{min}}(\mathrm{k}) \geq 0 \tag{27}$$

$$E_b(\mathrm{k}) \leq E_{b_{max}}(k) \quad , \quad E_{b_{min}}(\mathrm{k}) \geq 0 \tag{28}$$

$$SOC_{min}(\mathrm{k}) \leq \mathrm{SOC(k)} \leq SOC_{max}(k) \tag{29}$$

3.2. Modeling Renewable Energy Outputs: Wind and Solar Variability

The energy output from renewable sources, such as wind or solar, is intricately tied to the inherent characteristics of these sources [33]. The dynamic nature of wind speed underscores the importance of employing a probabilistic model, often represented by the Weibull distribution function:

$$f_v(v_t) = \begin{cases} \left(\frac{\beta}{c}\right) \cdot \left(\frac{v_t}{c}\right)^{k-1} .e^{\left(-\left(\frac{v_t}{c}\right)^k\right)} & vt \geq 0 \\ 0 & \end{cases} \tag{30}$$

Here, k and c denote the parameters of the Weibull distribution, and v represents the wind speed. To capture the hourly load outcome of a WT, the speed-power outcome curve is determined using the following formula:

$$P_{wt}^{t}=\begin{cases} P_{wt,r}, v_r < v^t < v_{cout} \\ P_{wt,r}\dfrac{v^t - v_{cin}}{v_r - v_{cin}}, v_{cin} < v^t < v_{cout} \\ 0, otherwise \end{cases} \tag{31}$$

Where P_{wt}^{t} is the WT generation capacity at t hour and $P_{wt,r}$ is the nominal WT generation capacity in KW. $v^t, v_r, v_{cin}, v_{cout}$, are respectively, wind speed at t-hour will be the nominal velocity, low cut-off speed and high cut-off speed in m / s.

The output capacity of a PV unit varies with solar radiation, influenced by factors such as environmental conditions, time of day, month, season, and the orientation of solar cells. The beta distribution function is employed to simulate solar radiation:

$$f\ (R_t) = \frac{\Gamma(\varphi,\zeta)}{\Gamma(\varphi).\Gamma(\zeta)}.R_t^{(\varphi-1)}.(1-R_t) \tag{32}$$

The φ,ζ are the selection parameters of beta. The power output of solar cells is contingent on the sunlight received by PV cells, and it is computed using the following equation:

$$P_{pv}^{t} = \eta_{pv} r^t S_{pv} \tag{33}$$

In which P_{pv}^{t} is power outcome of the PV system, η_{pv}, S_{pv} are efficiency and area of the PV cells and value of radiation reached per unit area per hour in t in KW, respectively. In summary, the power production for different scenarios and PV output is determined by Equations (13) and (14), respectively. WT output in each scenario is given by Equation (15), and the final power output is obtained using Equation (16).

3.3. Implementation Steps for Optimizing DDESS

In the context of this study, system implementation is intricately linked to control horizon and designated time horizon N, forming DDESS. The optimization of model structure involves a systematic series of steps, outlining the implementation of the system:

Determine Control Horizons: Define control horizon N_c and simulation time horizon N.

Update System Parameters: Update system parameters at a specified time instance denoted as k*.

Smart Meter Reading: Record smart meter readings of EF in various components outlined in Figure 1.

Update System Constraints: Adjust the system constraints at selected sample time as detailed in Step 2.

Implement DDESS Strategy: Employ the DDESS strategy using either equations (25) or (26).

Optimal EF: Determine optimal amount of EF.

Update Control Horizon: Update method control horizon, i.e., set updated kupdate = k* + 1.

Iterate System Process: Iterate through Steps 2 through 7 of the system process unless the duration of simulation horizon N is reached.

Create Optimal System Solution: Synthesize the optimal solution for the system.

This step-wise approach outlines the systematic execution of the DDESS, emphasizing the iterative nature of the optimization process to ensure a comprehensive and effective solution is obtained for the given time horizon.

4. Wild Mice Colony-Inspired Algorithm

Calhoun conducted research on a colony of mice in a laboratory environment, demonstrating that mice exhibit purposeful movements within colonies to adapt to their environment and ensure survival. In [34], the authors organized these behavioral results into an algorithm named after this organism. As a recently introduced foundational method, this algorithm's adaptive mechanism has the potential to address a wide array of problems, demonstrating its versatility in providing effective solutions. In this paper, we employ this framework to tackle complex problems. The parameters used for this algorithm are listed in Table 1.

Table 1. Parameters Used for the Algorithm

Parameter	Value/Formula
Number of Colonies	Arbitrary
Number of Male Mice	Number of Colonies * 4
Number of Female Mice	Number of Colonies * 8
Mouse Norm Value	Initial value 0.1
Age of Mice	Initial value 0.1
Acceptance of Female Mice	Initial value 0
Type of Mouse	Colony Head (CH) or Colony Member (CM)
Gender of Mouse	Male (M) or Female (F)
Reserve Colony	An empty array

The complete description of the algorithm's steps is as follows:

Initial Population Generation: Randomly, and within the problem space, a total of (number of colonies * 12) particles are generated. The population of these colonies is determined based on the initial parameters defined for the number of male and female mice. The number of male and female mice is randomly and proportionally determined according to the specified counts.

$$\begin{aligned}
&For\ i = 1\ to\ n\ Colony \times colonyNumber\\
&Mice(i) \cdot position = xmin + (xmax - xmin) \times rand(1, nvar);\\
&Mice(i) \cdot sec = m\\
&For\ i = 1\ to\ n\ Colony \times 8 Mice(i) \cdot position\\
&\qquad\qquad = xmin + (xmax - xmin) \times rand(1, nvar);\\
&Mice(i) \cdot sec = f
\end{aligned} \tag{34}$$

Initial Evaluation: To evaluate the initial randomly generated population, the initial population is placed in the cost function, and their fitness values are determined.

$$Mice(i) \cdot cost = Fitness\ (Mice(i) \cdot position) \tag{35}$$

Selection of the Most Normative Male Mice for Colony Formation: In the experiment conducted on mice, a principle observed among the mice was introduced as the "mouse norm". According to this norm, mice will recognize their hierarchical priority. In essence, mice with a higher norm are in a better position compared to other mice to establish colonies, mate, etc. The initial population is sorted based on the cost function, and the number of male mice equal to the number of colonies is selected from the beginning of this sorted array to establish their colonies or territories. The type parameter of these mice is changed to CH (Colony Head).

$$\begin{aligned}
&BestArray = Sort\ (Mice\ (i) \cdot cost)\\
&For\ i = BestArray\ (1)\ to\ BestArray\ (nColony)\\
&if\ mice\ (i) \cdot sec = m\\
&mice\ (i) \cdot Norm = mice\ (i) \cdot Norm + 1;\\
&mice\ (i) \cdot type = CH
\end{aligned} \tag{36}$$

Determination of Colony Members: These mice randomly select 3 male mice and 8 female mice from the population to be part of their colony.

$$if\ mice\ (i) \cdot type = CH \rightarrow Create\ [Colony\ (i)] \tag{37}$$

According to Calhoun's experiment, each colony will have 4 male members. Initially, a number of males will be identified from the population of each colony. Additionally, each colony will have 8 female members selected from the total 12 members of each colony.

$$\begin{aligned}
&[Colony\ (i).index] = rand\ [(mice.sec = m): mNumber]\ \&\\
&rand\ [(mice.sec = f): fNumber]
\end{aligned} \tag{38}$$

$$If\ \ Colony\ Member\ (i).Mcount \geq ColonyNumberExit \tag{39}$$

$$ColonyMmember(i).Fcount = ColonyMmember(i).Fcount + 1$$
$$if\ ColnyMember\ (i).Fcount \geq fNumber \tag{40}$$

According to the results obtained from the behavior of mice, it was found that the age of mice is important in their social interactions, so the age of mice will also be taken into account. The age of the mice is according to the relation (41) which is added by one unit in each iteration.

$$For\ i = 1\ to\ iteration$$
$$mice(i).age = mice(i).age + 1 \tag{41}$$

The higher the density of the colony, the lower the norm of the rats in that colony, and its relationship is formulated as (42).

$$if\ \left(Std \sum_{j=1}^{n} (mice(j).Position)\right) < Treshhold \quad mice(i).Norm = mice(i).norm - 1 \tag{42}$$

Movement of Mice: To adjust the location of each mouse during each evaluation, two different methods are used for regular colony members and colony heads:

1. Movement of Regular Colony Members: The movement of regular colony members is based on a random movement and the average location of mice within the same colony.
2. Movement of Colony Heads: The movement of colony heads is based on a random movement and the location of the best other colony head.

Mating of Male and Female Mice: To facilitate mating, the best colony head mouse (CH) is selected and mates with a female mouse whose acceptance parameter is set to one. The acceptance parameter of female mice is set to one under the following condition: the best female mouse in the colony will have its acceptance parameter set to one if it is in the mating round. Mating occurs three times a year. Colony head mice mate with female mice under three conditions, selected randomly, and produce between 5 to 15 new mice. The gender distribution of the newborn mice is determined randomly. The offspring compete with the young population of the same colony, and half of the weaker competing population is expelled from the colony.

Creation of New Colonies: The newborn mice compete with the young population of the same colony. Half of the weaker competing population is expelled from the colony (the expelled population goes to the reserve colony). The second-ranking member of a colony, being the most normative mouse after the colony head, attacks the most deviant colony in terms of location, kills half of the deviant colony's mice, and then establishes a new colony. Afterward, the population of that colony is sorted, and the second male after the colony head separates from the colony. This second male then attacks the most deviant colony head, kills half of the young population of that colony, and places the remaining members, along with any excess members from the colony where it was born, into the reserve colony. The attacking mouse then begins to establish a new colony. To create a new colony, the attacking mouse selects 8 females and 1 male from the reserve colony. If this number is not available, the colony will remain underpopulated until the next iteration, where any colony with a low population can request members from the reserve colony. This process of requesting and supplying members continues in each iteration if there is a shortage of members. The reserve colony does not actively participate in the problem space. In each iteration, colonies with a shortage of members recruit from the reserve colony. After the mating and movement actions, and in each iteration, the best overall optimizer of each colony is determined. Subsequently, the best overall optimizer of the entire population is identified. At the end of the final iteration, the best overall optimizer of the entire population is designated as the best solution.

Chaos Search: Utilizing the chaotic search method in intelligent algorithms presents a novel approach for addressing intricate problems characterized by non-linear functions. The chaotic method, grounded in non-linear and non-convex functions, has gained increased prominence. This paper provides a comprehensive review of the chaotic method as applied in existing literature and introduces a novel chaotic method designed to tackle the challenge of electricity price prediction. A pivotal equation derived from chaos theory is expressed as Equation (43) and can be formulated as follows:

$$c_{i+1}^{j} = \begin{cases} 2c_i^j, if \ \ 0 < c_i^j \le 0.5 \\ 2(1-c_i^j), if \ \ 0.5 < c_i^j \le 1 \end{cases}, j = 1, 2, ..., Ng \tag{43}$$

where c denotes chaotic particles in jth dimension and ith iteration; and Ng is defined as number of variables for optimization.

The Colony of Mice Algorithm incorporates several steps akin to other meta-heuristic algorithms. Below is a general breakdown and summary of the key steps:

Initialization: Generate an initial population of solutions, representing potential solutions to the optimization problem. In the context of the Colony of Mice Algorithm, these solutions are regarded as positions in the solution space.

Objective Function Evaluation: Evaluate the objective function for each solution in the population. The objective function measures the quality or fitness of each solution.

Behavior Analysis: Analyze the behaviors of the mice in the colony. This step involves observing and considering the individual or collective actions of mice, translating these behaviors into algorithmic operations.

Updating Positions: Update the positions of mice in the solution space based on their observed behaviors and the information gathered from the objective function evaluations. This step aims to guide the algorithm toward better solutions.

Local Search (Chaos): Perform local search operations around promising solutions. This involves exploring the local neighborhood of solutions to identify improvements.

Global Exploration: Encourage exploration of the solution space to discover new and potentially better solutions. This step may involve introducing randomness or diversity in the search process.

Termination Criteria: Check the termination criteria to determine whether the algorithm should stop. Termination criteria may include reaching a maximum number of iterations, achieving a satisfactory solution, or exceeding a defined computational budget.

Solution Update: Update the best-found solution if a new, better solution is discovered during the search process.

Iteration: Repeat steps 2-8 for a predefined number of iterations or until the termination criteria are met. Each iteration represents a cycle of the algorithm.

Output: Output the best solution found during the entire search process as the algorithm's result.

5. Simulation results and discussion

Tables 2 and 3 present crucial simulation values for the proposed DDESS, focusing on the DES system and the installed capacity of DG components such as PV panels and WTs [12]. $E_{d.avg}$ is derived from the daily average energy demand, and the maximum EF values for each component are constrained by a function based on the maximum energy demand. The strategy operates on the assumption that the energy production system can independently meet the demand. For DG, the maximum values for PV and WTs are initially set to their capacities, but for optimal exploration, these are later assumed to align with the maximum energy demand. This approach ensures a thorough examination of the system's capabilities, emphasizing the interplay between energy production and demand in the proposed DDESS framework. The simulation was conducted on a personal computer equipped with an Intel 5-core processor and 16 gigabytes of RAM. The program's execution time was less than 2 minutes, which is considered acceptable for computations within the sub-network.

Table 2. Simulation parameters

Parameters	**Values**	**Parameters**	**Values**
SOC_{max}, %	94	n_{inv}, %	90
SOC_{min}, %	45	Ha, h	5
n_{ch}, %	90	P_{pv}, kW	5
n_{disc}, %	90	P_{wt}, kW	1.5

Table 3. Energy demand, average of wind speed velocity and solar irradiance

Time	Energy Demand (kWh)	Average Wind Speed (m/s)	Solar Irradiance (W/m2)
00:00	0.6	0.82	0
01:00	1.72	1.665	0

02:00	0.46	0.998	0
03:00	0.9	0.956	0
04:00	2.18	2.549	0
05:00	5.72	2.558	0
06:00	6.98	2.775	15.418
07:00	4.82	3.754	119.344
08:00	1.44	2.948	233.282
09:00	4.24	2.828	336.534
10:00	1.16	2.87	438.693
11:00	4.6	2.522	482.247
12:00	0.84	1.766	494.023
13:00	0.62	2.576	472.315
14:00	0.56	2.017	418.492
15:00	4.34	2.282	308.193
16:00	7.02	3.116	198.642
17:00	2.82	2.626	82.118
18:00	2.48	3.427	4.934
19:00	8.48	2.972	0
20:00	3.66	2.543	0
21:00	3	2.336	0
22:00	2.58	1.863	0
23:00	0.68	1.231	0

The simulation outcomes for the devised DDESS system are illustrated in Figures 3 to 8. These results are obtained by examining various initial SOC values of the battery. To assess the SPI and energy savings, eight distinct initial SOC values—90%, 85%, 80%, 75%, 70%, 65%, 60%, and 55%, as specified in Table 2—are chosen. It is important to note that these values are normalized by dividing them by 100 to present a unified range in Figures 3 to 8, preventing label congestion. Figures 3 to 8 illustrate the optimal results for DG, encompassing PV and WT components, considering various SOC values. In Figure 3, the initial four configurations (0.950, 0.850, 0.800, and 0.750) showcase the efficient EF from PV. These configurations demonstrate optimal PV production patterns, emphasizing instances where the production serves either the consumer load (battery) or directly benefits the consumer. A similar comparative analysis is extended to the WT in Figure 4.

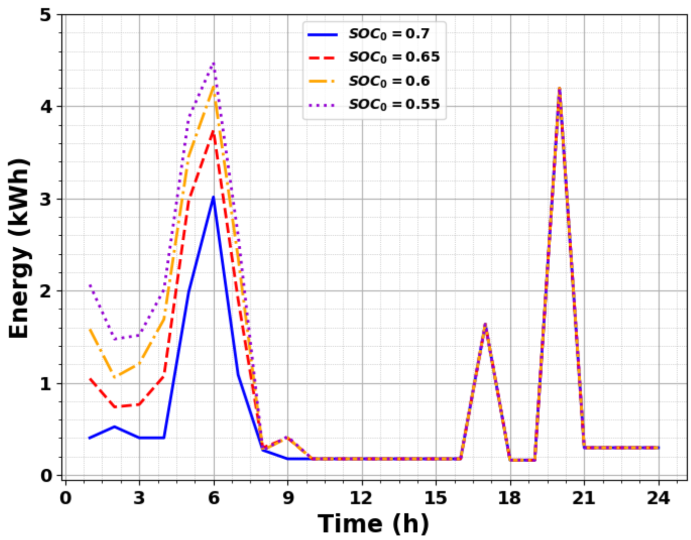

Figure 3: Optimum flow from the PG (energy supply from the PG)

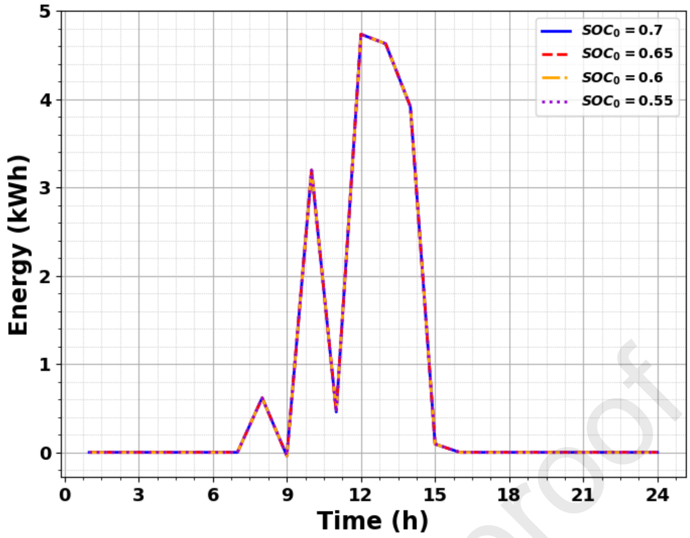

Figure 4: Optimum current from the PG (BESS charging)

Moreover, Figure 5 elucidates the optimal EF patterns in PV systems for the remaining four initial battery SOC values: 0.70, 0.65, 0.60, and 0.55. These profiles are systematically compared with the energy generated by PV when it is not actively supplying any load. This comprehensive analysis offers insights into the dynamic behavior of the system under diverse battery SOC scenarios, providing a nuanced understanding of the interplay between PV production, energy storage, and load demands.

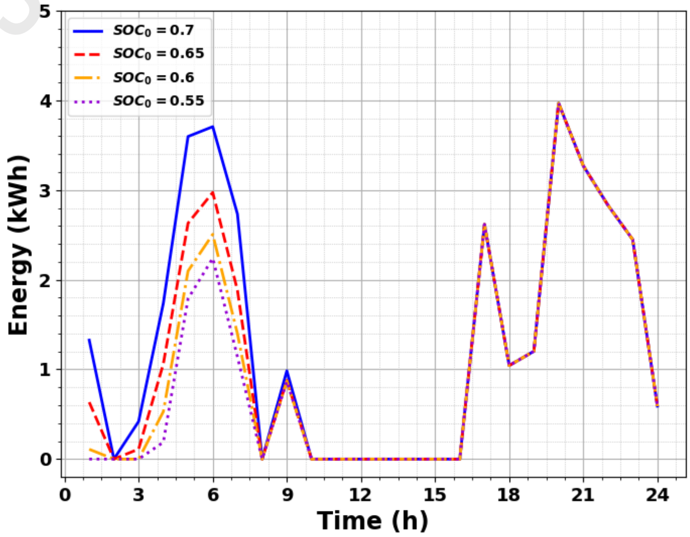

Figure 5: Optimum EF from PG (BESS discharge to load)

In Figure 6, a parallel approach is employed to illustrate the EF dynamics associated with the WT. Notably, the EF patterns for DG exhibit a consistent pattern across different battery SOC values, as depicted in the figure. This consistency underscores the system's resilience in harnessing energy from renewable sources. The observation suggests that there is minimal energy loss in the DG component, emphasizing a balanced equilibrium wherein the energy generated aligns closely with the consumption requirements of either the consumer or the producer (battery storage). This cohesiveness underscores the efficiency of the system in optimizing energy utilization from renewable sources without unnecessary wastage.

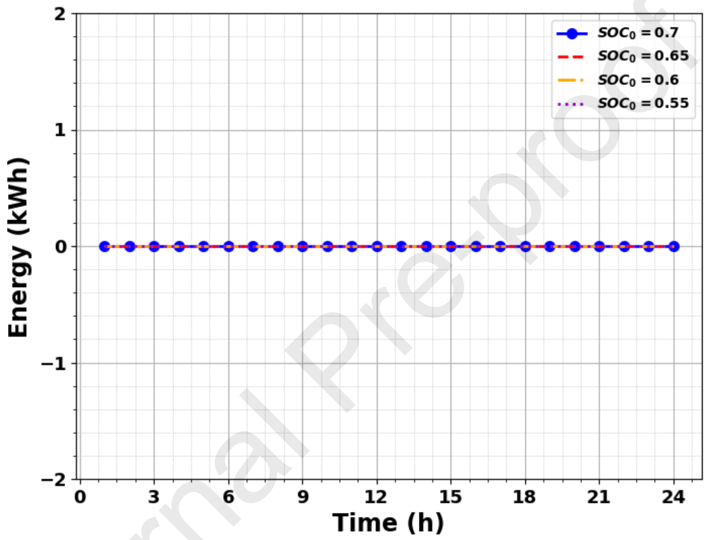

Figure 6: Optimum EF from PG

Figures 7 and 8 illustrate the behavior of the system across various initial SOC values, encompassing the entire spectrum between the maximum and minimum SOC limits of the battery. The implemented DDESS system exhibits robust performance, ensuring optimal EF within the residential sector under the smart grid framework. This model empowers consumers to fine-tune their EC patterns by strategically minimizing reliance on the PG, thereby contributing to enhanced EE within the smart grid paradigm.

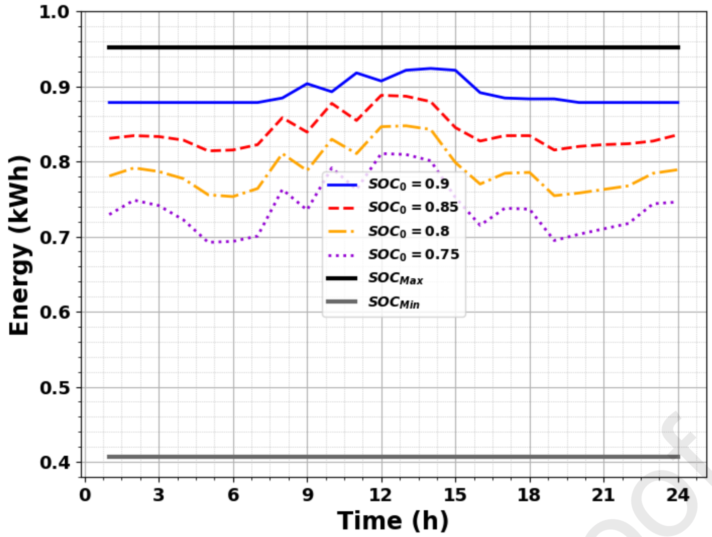

Figure 7: Battery with four initial SOC values

Examining Figures 7 and 8 reveals that the optimal energy storage solution intricately correlates with the probability distribution of the SPI. The interplay between the availability of opportunity energy and the SOC pattern indicates that even within the range of 74.65% to 56.74% initial SOC, there exists an opportunity for energy optimization. However, the optimal solution strategically avoids generating opportunity energy, underscoring the system's emphasis on maintaining robustness. Notably, this outcome is contingent upon battery parameters such as capacity and hourly discharge rates. It becomes evident that augmenting battery capacity could potentially unlock greater energy optimization opportunities within the system, albeit at the expense of requiring a more substantial investment in RERs. Consequently, the effectiveness of the energy and cost-saving system—allowing consumers to offset PG expenses—is intimately tied to the initial SOC value of the BESS. A higher initial SOC, closer to the maximum SOC, yields significant savings, while a lower initial SOC, approaching the minimum SOC, diminishes the potential for cost reduction. This nuanced relationship underscores the importance of considering the initial SOC as a pivotal factor in optimizing energy and cost outcomes within the system.

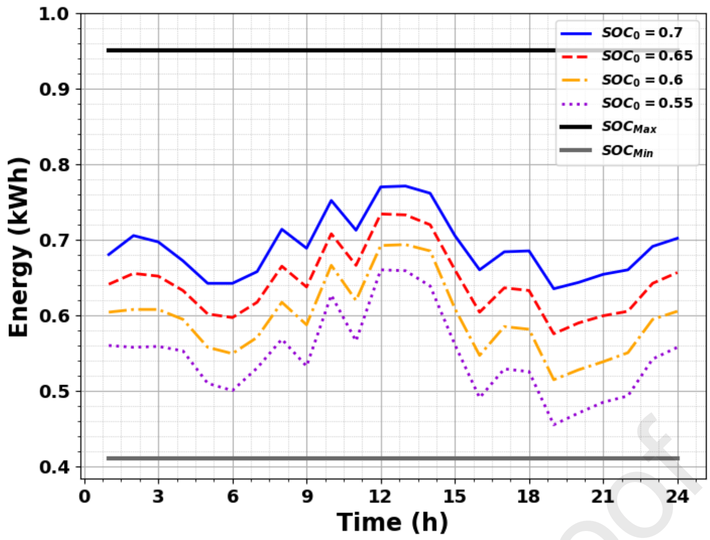

Figure 8: Battery with the last four SOC values

In addition, Table 4 shows the OCM behavior of the intelligent switching system. Various switching devices, namely S1 to S6, are provided. Consumer Energy Payback (CEPB) and Consumer End Energy Payback (CEEPB) denote crucial energy cost indicators. The findings from the DDESS are meticulously analyzed and summarized in Tables 5 and 6. Table 4, focusing on end-user EC analysis, underscores a pivotal range between set points 0.9 and 0.85, where the CEEPB demonstrates significant positive values, signifying potential benefits for the end user. However, as the set points drop to values between 0.80 and 0.550, CEEPB values turn negative. In contrast to N-Energy, these negative amounts indicate the minimum EC threshold at which the consumer can compensate the supplier. This nuanced exploration of energy cost metrics provides valuable insights into the dynamic interplay between set points and end-user energy payback, guiding optimal decision-making within the DDESS framework.

Table 4. Intelligent switching system of dynamic distributed energy storage system based on residential energy coordination

Time (h)	S1	S2	S3	S4	S5	S6
1	0	1	0	1	0	1
2	0	1	0	1	0	1
3	0	1	0	1	0	1
4	0	1	0	1	0	1
5	0	1	0	1	1	0
6	0	1	0	1	1	0
7	1	1	0	1	1	0
8	1	1	1	0	0	1
9	1	1	0	1	0	1
10	1	1	1	0	0	1

11	1	1	1	0	0	1
12	1	1	1	0	0	1
13	1	1	1	0	0	1
14	1	1	1	0	0	1
15	1	1	0	1	0	1
16	1	1	0	1	1	0
17	1	1	0	1	0	1
18	1	1	0	1	1	1
19	1	1	0	1	1	0
20	0	1	0	1	0	1
21	0	1	0	1	0	1
22	0	1	0	1	0	1
23	0	1	0	1	0	1
24	0	1	0	1	0	1

The tables provide a comprehensive overview of EC and cost analyses under different scenarios, each reflecting variations in SOC percentages. Based on Table 5, the CEEPB in kWh demonstrates intriguing patterns. At higher SOC percentages (90% and 85%), there is a positive CEEPB, indicating a surplus of energy that can be beneficial for the end user. However, as the SOC decreases, CEEPB turns negative, suggesting a deficit in energy supply. This trend aligns with expectations, as lower SOC values imply reduced energy availability for the consumer. Based on Table 6, the saving percentages and cost analyses in scenario 1 highlight the economic implications of EC. As SOC decreases, the savings percentages fluctuate. Notably, at higher SOC (90% and 85%), there is a substantial positive saving percentage, indicating potential cost savings for the end user. However, as SOC decreases, the savings turn negative, suggesting increased costs for the consumer. Based on Table 7, scenario 2 presents a similar trend, with varying saving percentages and cost analyses. The positive savings percentages at higher SOC values suggest cost-effective EC. Conversely, lower SOC values correlate with negative savings, indicating increased costs.

Higher SOC values result in positive CEEPB, reflecting surplus energy. Conversely, lower SOC values lead to negative CEEPB, indicating a shortage. The transition from surplus to deficit aligns with expectations. Both scenarios exhibit a similar pattern. Higher SOC values coincide with positive savings percentages, indicating potential cost savings, while lower SOC values are associated with negative savings, signifying increased costs. The analysis underscores the critical role of SOC in influencing both energy availability and associated costs. Higher SOC values provide a buffer for cost-effective EC, while lower SOC values result in increased expenses. This insight aids in optimizing energy utilization and cost management within the DDESS framework.

Table 5. Analysis of energy consumption

SOC %	**N-Energy** kWh	**O-Energy** kWh	**CEPB** kWh	**CEEPB** kWh
90	71.8	9.26	50.54	41.13
85	71.8	9.26	22.35	13.03
80	71.8	9.27	8.28	-0.98
75	71.8	9.34	0	-9.35
70	71.8	16.12	0	-16.18
65	71.8	21.11	0	-21.02
60	71.8	24.87	0	-24.32
55	71.8	27.86	0	-27.56

Table 6. Energy consumption cost analysis scenario 1

SOC %	**N-Cost** (R)	**O-Cost** (R)	**CEPB** (R)	**CEEPB** (R)
90	87.56	11.21	32.56	21.32
85	87.56	11.34	14.21	3.56
80	87.56	11.33	5.34	-5.64
75	87.56	11.13	0	-11.02
70	87.56	19.56	0	-19.42
65	87.56	25.48	0	-24.85
60	87.56	30.25	0	-30.21
55	87.56	34.32	0	-34.02

Table 7. Energy consumption analysis scenario 2

SOC %	**N-Cost** R)(	**O-Cost** (R)	**CEPB** (R)	**CEEPB** (R)
90	88.32	11.52	62.15	50.58
85	88.32	11.52	28.18	16.21
80	88.32	11.52	9.96	-1.09
75	88.32	11.68	0	-11.80
70	88.32	19.82	0	-18.95
65	88.32	26.02	0	-26.03
60	88.32	31.05	0	-31.14
55	88.32	33.92	0	-33.91

6. Conclusion

The simulation and analysis of the Dynamic Distributed Energy Storage System (DDESS) yield several critical insights, aligning with the paper's focus on optimizing residential energy management within the smart grid framework:

1. **System Resilience and Efficiency:** The DDESS exhibits robust performance in aligning energy production with demand variations throughout the day. By leveraging optimal operation strategies, the system maximizes Energy Flow (EF) across different battery State of Charge (SOC) scenarios. Figures 3 to 8 demonstrate that the system dynamically adjusts the energy flow from Photovoltaic (PV) and Wind Turbine (WT) components to meet consumer load requirements, minimizing reliance on the Power Grid (PG) and ensuring minimal energy wastage. This resilience underscores the system's capability to harness renewable energy effectively.

2. **Economic and Energy Benefits:** The cost analysis presented in Tables 5 to 7 highlights the significant economic benefits of maintaining higher SOC levels within the battery. Higher SOC values correlate with positive Consumer End Energy Payback (CEEPB) and cost savings, while lower SOC values lead to increased costs due to reduced energy availability. This finding emphasizes the importance of optimizing battery SOC to enhance energy consumption efficiency and reduce costs within residential settings. The intelligent switching system further enhances operational flexibility, facilitating real-time adjustments in energy consumption patterns to respond to fluctuating energy demands and availability from Renewable Energy Sources (RES).

3. **Enhanced Energy Security and Sustainability:** The DDESS's ability to integrate and optimize renewable energy sources contributes significantly to the smart grid framework. By empowering consumers to manage their energy consumption more efficiently, the system enhances energy security and supports sustainable energy practices. This integration reduces dependency on conventional power sources, aligning with the goal of promoting environmentally friendly energy solutions.

4. **Alignment with Smart Grid Paradigms:** The findings underscore the pivotal role of DDESS in modern energy management paradigms. By optimizing energy utilization from renewable sources and providing substantial benefits in terms of energy efficiency and cost savings, the DDESS contributes to the advancement of smart grid technologies. This system's capability to dynamically balance energy supply and demand, coupled with its economic advantages, makes it a valuable asset for policymakers, energy planners, and residential consumers.

Here, the DDESS demonstrates its potential to revolutionize residential energy management by optimizing energy flows, enhancing economic efficiency, and supporting sustainable energy practices. These insights are crucial for stakeholders aiming to adopt resilient and environmentally friendly energy solutions, aligning with the broader objectives of modern smart grid initiatives.

This study has several limitations that warrant future research. The proposed Dynamic Distributed Energy Storage Strategy (DDESS) is primarily tested in residential settings, and its scalability to commercial or industrial applications remains unexamined. The Wild Mice Colony (WMC) optimization algorithm, while innovative, may face computational challenges that could impact real-time use, suggesting a need for further optimization. Additionally, the model assumes static pricing, which may not capture real-world dynamic pricing variations; integrating adaptive pricing mechanisms could improve accuracy. The study also does not account for battery degradation over time, which could affect long-term system performance. Future research should address these limitations to enhance the model's applicability and effectiveness in diverse energy management scenarios.

Funding:

Not applicable.

Data Availability:

Not applicable.

Conflict of interest:

The authors declare that they have no known competing financial interests or personal relationships that could have appeared to influence the work reported in this paper.

Human Participants and/or Animals:

Not applicable.

Ethical approval:

Not applicable.

Acknowledgment:

Not applicable.

Reference

[1] Wang, Yubin, Wei Dong, and Qiang Yang. "Multi-stage optimal energy management of multi-energy microgrid in deregulated electricity markets." Applied Energy 310 (2022): 118528.

[2] Kalani, Mohammad Javad, and Mahdi Kalani. "Controlling the energy supply and demand of grid-connected building integrated photovoltaics considering real-time electricity prices to develop more sustainable and smarter cities." Optik 300 (2024): 171629.

[3] Huang, Z. F., Chen, W. D., Wan, Y. D., Shao, Y. L., Islam, M. R., & Chua, K. J. (2024). Techno-economic comparison of different energy storage configurations for renewable energy combined cooling heating and power system. Applied Energy, 356, 122340.

[4] Khosravani, Ali, et al. "Electrification of residential and commercial buildings integrated with hybrid renewable energy systems: A techno-economic analysis." Energy (2024): 131893.

[5] Ren, Kezheng, et al. "A data-driven DRL-based home energy management system optimization framework considering uncertain household parameters." Applied Energy 355 (2024): 122258.

[6] Youssef, Heba, et al. "An improved bald eagle search optimization algorithm for optimal home energy management systems." Soft Computing 28.2 (2024): 1367-1390.

[7] Abedinia, Oveis, et al. "Presence of renewable resources in a smart city for supplying clean and sustainable energy." Decision making using AI in energy and sustainability: methods and models for policy and practice. Cham: Springer International Publishing, 2023. 233-251.

[8] Abdel-Basset, M., Gamal, A., Hezam, I. M., & Sallam, K. M. (2024). Sustainability assessment of optimal location of electric vehicle charge stations: a conceptual framework for green energy into smart cities. Environment, Development and Sustainability, 26(5), 11475-11513.

[9] F. Luo, G. Ranzi, W. Kong, Z. Y. Dong, and F. Wang, "Coordinated residential energy resource scheduling with vehicle-to-home and high photovoltaic penetrations," *IET Renewable Power Generation*, vol. 12, no. 6, pp. 625-632, 2018.

[10] A. Anvari-Moghaddam, H. Monsef, and A. Rahimi-Kian, "Optimal smart home energy management considering energy saving and a comfortable lifestyle," *IEEE Transactions on Smart Grid,* vol. 6, no. 1, pp. 324-332, 2014.

[11] X. Chen, J. Wang, J. Xie, S. Xu, K. Yu, and L. Gan, "Demand response potential evaluation for residential air conditioning loads," *IET Generation, Transmission & Distribution,* vol. 12, no. 19, pp. 4260-4268, 2018.

[12] Lokeshgupta, B., & Ravivarma, K. (2023). Coordinated smart home energy sharing with a centralized neighbourhood energy management. Sustainable Cities and Society, 96, 104642.

[13] Shen, Hanfeng. "Planning of renewable energy regional heating system based on demand side uncertainty." Results in Engineering 22 (2024): 101997.

[14] Berouine, A., Ouladsine, R., Bakhouya, M., & Essaaidi, M. (2022). A predictive control approach for thermal energy management in buildings. Energy Reports, 8, 9127-9141.

[15] D. Tungadio, R. Bansal, M. Siti, and N. Mbungu, "Predictive active power control of two interconnected microgrids," *Technology and Economics of Smart Grids and Sustainable Energy,* vol. 3, pp. 1-15, 2018.

[16] Zou, B., Peng, J., Yin, R., Luo, Z., Song, J., Ma, T., ... & Yang, H. (2023). Energy management of the grid-connected residential photovoltaic-battery system using model predictive control coupled with dynamic programming. Energy and Buildings, 279, 112712.

[17] M. Amini, J. Frye, M. D. Ilić, and O. Karabasoglu, "Smart residential energy scheduling utilizing two stage mixed integer linear programming," in *2015 North American Power Symposium (NAPS)*, 2015, pp. 1-6: IEEE.

[18] A. Safdarian, M. Fotuhi-Firuzabad, and M. Lehtonen, "Optimal residential load management in smart grids: A decentralized framework," *IEEE Transactions on Smart Grid,* vol ,7 .no. 4, pp. 1836-1845, 2015.

[19] Sun, Yiyun, et al. "Energy management based on safe multi-agent reinforcement learning for smart buildings in distribution networks." Energy and Buildings (2024): 114410.

[20] M. Martinez-Pabon, T .Eveleigh, and B. Tanju, "Optimizing residential energy management using an autonomous scheduler system," *Expert Systems with Applications,* vol. 96, pp. 373-387, 2018.

[21] R. Bansal, "Handbook of distributed generation," *Electric Power Technologies, Economics and Environmental Impacts,* vol. 11, p. 6330, 2017.

[22] F. Y. Melhem, O. Grunder, Z. Hammoudan, and N. Moubayed, "Optimization and energy management in smart home considering photovoltaic, wind, and battery storage system with integration of electric vehicles," *Canadian Journal of Electrical and Computer Engineering,* vol. 40, no. 2, pp. 128-138, 2017.

[23] Y. Guo, M. Pan, Y. Fang, and P. P. Khargonekar, "Decentralized coordination of energy utilization for residential households in the smart grid," *IEEE transactions on smart grid,* vol. 4, no. 3, pp. 1341-1350, 2013.

[24] Y. Liu, C. Yuen, R. Yu, Y. Zhang, and S. Xie, "Queuing-based energy consumption management for heterogeneous residential demands in smart grid," *IEEE Transactions on Smart Grid,* vol ,7 .no. 3, pp. 1650-1659, 2015.

[25] S. Arun and M. Selvan, "Intelligent residential energy management system for dynamic demand response in smart buildings," *IEEE Systems Journal,* vol. 12, no. 2, pp. 1329-1340, 2017.

[26] M. Rastegar, M. Fotuhi-Firuzabad ,H. Zareipour, and M. Moeini-Aghtaieh, "A probabilistic energy management scheme for renewable-based residential energy hubs," *IEEE Transactions on Smart Grid,* vol. 8, no. 5, pp. 2217-2227, 2016.

[27] T. Alquthami and A. S. Meliopoulos, "Smart house management and control without customer inconvenience," *IEEE Transactions on Smart Grid,* vol. 9, no. 4, pp. 2553-2562, 2016.

[28] M. H. Barmayoon, M. Fotuhi-Firuzabad, A. Rajabi-Ghahnavieh, and M. Moeini-Aghtaie, "Energy storage in renewable-based residential energy hubs," *IET Generation, Transmission & Distribution,* vol. 10, no. 13, pp. 3127-3134, 2016.

[29] X. Wu, X. Hu, X. Yin, and S. J. Moura, "Stochastic optimal energy management of smart home with PEV energy storage," *IEEE Transactions on Smart Grid,* vol. 9, no. 3, pp. 2065-2075, 2016.

[30] N. T. Mbungu, R. C. Bansal, and R. Naidoo, "Smart energy coordination of a hybrid wind/PV with battery storage connected to grid," *The Journal of Engineering,* vol. 2019, no. 18, pp. 5109-5113, 2019.

[31] T. Sayfutdinov, C. Patsios, J. W. Bialek, D. M. Greenwood, and P. C. Taylor, "Incorporating variable lifetime and self-discharge into optimal sizing and technology selection of energy storage systems," *IET smart grid,* vol. 1, no. 1, pp. 11-18, 2018.

[32] N. Mbungu" ,Dynamic real time electricity pricing optimisation for commercial building," *MEng: Department of Electrical, Electronic and Computer Engineering, University of Pretoria, South Africa,* 2017.

[33] Y. Khawaja, D. Giaouris, H. Patsios, and M. Dahidah, "Optimal cost-based model for sizing grid-connected PV and battery energy system," in *2017 IEEE Jordan Conference on Applied Electrical Engineering and Computing Technologies (AEECT)*, 2017, pp. 1-6: IEEE.

[34] Nejatian, S., Omidvar, R., Parvin, H., Rezaei, V., & Yasrebi, M. (2019). A new algorithm: wild mice colony algorithm (WMC). Tabriz Journal of Electrical Engineering, 49(1), 425-437.

Declaration of interests

☒ The authors declare that they have no known competing financial interests or personal relationships that could have appeared to influence the work reported in this paper.

☐The authors declare the following financial interests/personal relationships which may be considered as potential competing interests: